Optica Applicata, Vol. XXXV, No. 4, 2005

Restoration and fusion optimization scheme of multifocus image using genetic search strategies

XINMAN ZHANG*, JIUQIANG HAN, PEIFEI LIU

School of Electronics and Information Engineering, Xi'an Jiaotong University,
28 Xian'ning West Road, Xi'an 710049, People' s Republic of China

*Corresponding author: Xinman Zhang, ccp9999@sina.com.cn

A novel and optimal algorithm is presented that is suitable for multifocus image fusion. A synergistic combination of segmentation techniques and genetic search strategies is employed in salience analysis of contrast feature-vision system. Some evaluation measures are suggested and applied to compare the performance of different fusion schemes. Two cases of the generated test images are discussed and extensive experiments demonstrate that in one case most fused images achieve reconstruction or optimized effects with respect to the reference image when the focus objectives are not overlapped blurred, and in the other case this method produces better results outperforming other conventional methods when the focus objectives are overlapped blurred. It is therefore shown that the performance of the fusion algorithm proposed optimizes further the fused image globally accomplishing absolute restoration or optimized fusion of multifocus image to the reference image. This algorithm is also suitable for the digital camera images of real scene and gets to be optimized well.

Keywords: multifocus image fusion, genetic search strategies, zero reconstruction error, contrast feature -vision system.

1. Introduction

Image fusion may be used to combine images from different sensors to obtain a single composite with extended information content. Fusion may also be used to combine multiple images from a given sensor to form a composite image in which information of interest is enhanced [1]. Multifocus image fusion is one kind of image fusion. It can be used to produce a fused image in which all relevant objects appear hopefully in focus so as to reduce blurring and remove obstructions in source images. The result of image fusion is a single image which is more suitable for human visual and machine perception or further image-processing tasks.

There are different methods available to implement multifocus image fusion. In recent years, many researchers recognize that multiscale transforms are very useful

for analyzing multifocus image fusion. The basic idea is to perform a multiscale transform on each source image, then construct a composite multiscale representation from these. The fused image is obtained by taking an inverse multiscale transform. Some sophisticated image fusion approaches based on multiscale representations begin to receive increased attention, such as Laplacian pyramid [2, 3], RoLP pyramid [4, 5], gradient pyramid [6] and steerable pyramid [7], *etc*. More recently, wavelet transform [8–13] and neural network [14, 15] fusion algorithms have emerged rapidly and performed satisfactorily. But these methods have some small errors when comparing the fused image with the reference image.

The novel approach proposed differs in a block-based fusion scheme, which leads, on the one hand, to the necessity of formulating the problem of analysing contrast feature-vision system, and on the other hand, to the integration of segmentation techniques and genetic block search scheme. A more lucid discussion of the existing work can be provided as far as our framework for image fusion is concerned. In the approach we studied, the fusion is performed without assuming any statistical properties of the observed images and does not require a priori knowledge. To verify the algorithm, dozens of multifocus images are producted, with the main emphasis being placed on "test images" and "digital camera images". We discuss in detail two cases of comparison analysis of the "test images". This paper is one of the first to consider zero reconstruction error for multifocus images when the focus objectives are not overlapped blurred. This new scheme is found to outperform other conventional schemes in both cases of interest.

This paper is organized as follows. Section 2 introduces data preparation for multifocus images. Section 3 presents a detailed algorithm and a schematic diagram, followed by measures we suggest in the next section. In Sections 5 and 6, two cases of multifocus images are discussed and the results are reported. Section 7 provides some important discussion. The last section summarizes the paper and the conclusions are finally drawn.

2. Data preparation

Assessing quantitatively the performance of image fusion in practical applications is a complicated task because the ideal composite image is normally unknown. One way of achieving this in a controlled setting is to generate pairs of distorted source images from a known test image, then compare the fused image and the original test image. This approach is reasonable to judge performance for cases where the source images come from the same type of sensors, which is our focus here. From a test image, two out-of-focus images are created by blurring with a Gaussian radius when we selected a focus object of an image. Then we get a pair of different accurately registered focus images with the corresponding pixels aligned.

Another case is the generated images acquired by a camera of different focal depths of the two images. Because the images may be misregistered and therefore may not be ideal, we may carry out some subjective visual evaluation.

3. Multifocus image fusion scheme-based genetic search

The goal in multifocus image fusion is to capture and preserve in a single output image all the "clear" part that is present within two input images. The basic fusion algorithm will be described in Section 3.1. In this section, the algorithm first decomposes the source images into blocks. Then, fusion proceeds by selecting a clearer block according to a uniform parameter. Section 3.2 describes the genetic search strategies. This section solves the problem of choosing a block size that optimizes the fused image furthest. Section 3.3 discusses the influence of the fitness function, *i.e.*, spatial frequency, on the fused image clarity.

3.1. Basic algorithm

According to Weber's law, in a uniform background I, the visible detection threshold of objects (contrast sensitivity threshold) ΔI is given by

$$\Delta I = 0.02 I. \tag{1}$$

Consider a contrast vision system, whose contrast sensitivity threshold is directly proportional to the background brightness [16]. The image block in varying pixels is considered as an overlapped varying signal in a uniform background. The signal range must attain certain intensity (detection threshold), so it is to be seen by the vision system. If the overlapped signal range is less than the detection threshold of the vision system, the image block is considered well-proportioned. The more intensive the background luminance is the more overlapped the signal intensity. This is called a contrast masking effect. In other words, with regard to the uniform image block, when the luminance is greater, the pixel variation in the block is larger.

Note that this visual information association is supported by human visual system studies and is extensively used in multifocus images. Thus, we address uniform parameter to test the definition of focus images which is more optimal than block variance, which represents deviations between the block pixel and the block mean. We shall treat an image as a two-dimensional array of pixels, and the pixel in the i-th row and the j-th column shall be denoted by $I(i, j)$. Using this notation, we define d_k, namely, the uniform parameter of partition block of an image I as follows:

$$d_k = \frac{1}{m' \times n'} \sum_{(i,j) \in B_k} \frac{\left| I(i,j) - \mu_k \right|}{\mu_k} \tag{2}$$

where μ_k is the mean of block B_k, and $m' \times n'$ is the block size. This paper adopts contrast to measure varying visibility of block signal improving the matching extent between segmentation process and vision system.

In the following, we shall assume that there are two out-of-focus inputs A and B. The fusion algorithm breaks up both of them into smaller square regions, *i.e.*, $m' \times n'$ blocks. Denote the i-th image block pair by BA_i and BB_i.

Then image fusion is performed based on uniform parameter of each block. The i-th block BF_i of the fused image is then constructed as

$$BF_i = \begin{cases} BA_i & \mathrm{d}A_i \geq \mathrm{d}B_i \\ BB_i & \text{otherwise} \end{cases} \tag{3}$$

where $\mathrm{d}A_i$ and $\mathrm{d}B_i$ are uniform parameters of the relative blocks BA_i and BB_i of two input images A and B, respectively. Given two of these blocks (one from each source image), the contrast vision model is to determine which one is clearer.

Next, each partition block is incorporated according to Eqs. (2) and (3), so the legible regions are selected and this process yields a merged image F. If the same object appears more distinct (in other words, with better contrast), in image A than B, after fusion the object in image A will be preserved, while the object in image B will be ignored.

3.2. Genetic search optimized algorithm

Image fusion is carried out as the key step, that is, the most important, to search the desired fused image in terms of different block sizes. Fusion then proceeds by selecting a clearer block in constructing the final image.

Genetic algorithms (GA) are search procedures based on the mechanics of natural selection and natural genetics [17, 18]. Having been established as a valid approach to problems requiring effective search, GA are now finding more widespread application in business, scientific, and engineering circles. These algorithms are computationally simple yet powerful in their search for improvement. Furthermore, they are not fundamentally limited by restrictive assumptions about the search space (assumptions concerning continuity, existence of derivatives, unimodality and other matters).

Here, we have proposed a genetic algorithm in image block search and have a good effect. The proposed method, relying on some genetic search factors, is a novel attempt to apply concepts coming from genetics to image processing, especially to multifocus images.

If we consider two sources A and B as the input images to be fused, the GA method can be applied to achieve this. The fusion optimization problem that we examine here can be considered as a search problem. The optimized image is chosen by employing a different combination of image blocks according to the adaptive genetic search algorithm.

The genetic strategy consists of the following steps:

1. Determine proper reference genus numbers N by stochastic method to produce a reference genus. The most optimized block size is likely to be chromosome number. Suppose that for an $M \times M$ image, the search range is $(0, M)$ for simplicity, so chromosome C_i of number i is composed of two parts representing blocks' length and width code;

$$C_i = \left[n'_{i,\,l-1}\ n'_{i,\,l-2}\ \ldots\ n'_{i,\,l/2+1}\ n'_{i,\,l/2}\ m'_{i,\,l/2-1}\ m'_{i,\,l/2-2}\ \ldots\ m'_{i,\,1}\ m'_{i,\,0} \right]$$

where l refers to chromosome code length (of size $2\log_2 M$) [19], and i belongs to the range $[0, N-1]$.

2. Compute the fitness function of each chromosome. Here, we consider the spatial frequency, *i.e.*, *SF* a detailed discussion of which is given in Section 3.3. With a bigger *SF* value, the corresponding chromosome is even more excellent. And the chance to produce offspring is higher.

3. Choose the most excellent chromosome copy directly for the next generation, and thus make it have more chances to reproduce new chromosomes. This can improve the speed of excellent individual control of genus numbers ameliorating local searching. Reproduction is a process in which individual strings are copied according to the fitness function. Intuitively, we can think of the function as some measure of profit, utility, or goodness that we want to maximize. Copying strings according to their fitness values means that strings with a higher value are probable to contribute one or more offspring in the next generation. Once a string has been selected for reproduction, an exact replica of the string is made. Choosing the N genus numbers and entering into a mating pool, a tentative new population, enables further genetic operator action.

4. Crossover: according to the crossover ratio P_c, the random partnership chromosomes and random exchanging positions, a new position of the search space is permitted to be tested. Crossover enables the exchange of information in nature.

5. Mutation: mutation is the occasional (with a small probability) random alteration of the value of a string position. In the binary coding of the black box problem, this simply means changing a 1 to a 0 and *vice versa*. So, a new population is produced. Through mutation operation, ensuring the diversity of gene types, it is possible to search more space avoiding losing useful information, to acquire the optimal answer of high quality.

6. Perform genetic folding operation; if the terminate condition is met, end the operation, if not, go to the next step. Here, the terminate condition is satisfied when the folding operation time equals $2\log_2(M/2)$.

7. Choose the optimized blocks to reach the best effect.

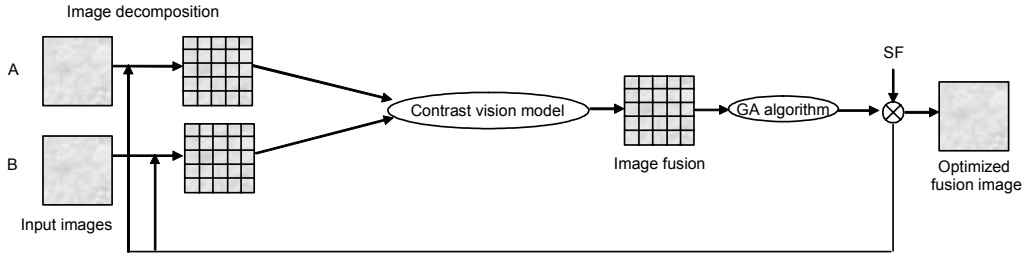

Fig. 1. Block diagram of the proposed multifocus image fusion scheme.

Figure 1 illustrates the block diagram of the proposed multifocus image fusion scheme.

3.3. Discussion of spatial frequency

The spatial frequency for a fused image is defined as follows. The row and column frequencies are given by

$$RF = \sqrt{\frac{1}{m \times n} \sum_{i=1}^{m} \sum_{j=2}^{n} \left[F(i,j) - F(i,j-1) \right]^2}$$

and

$$CF = \sqrt{\frac{1}{m \times n} \sum_{j=1}^{n} \sum_{i=2}^{m} \left[F(i,j) - F(i-1,j) \right]^2}$$

The total frequency is then

$$SF = \sqrt{RF^2 + CF^2} .$$

The definition of frequency in the spatial domain indicates the overall activity level in an image. At the same time it represents minus details of contrast and texture commutation characteristic. Generally, a larger *SF* value is referred to more activity and clarity.

Here, the effectiveness of *SF* in representing image clarity will be experimentally demonstrated.

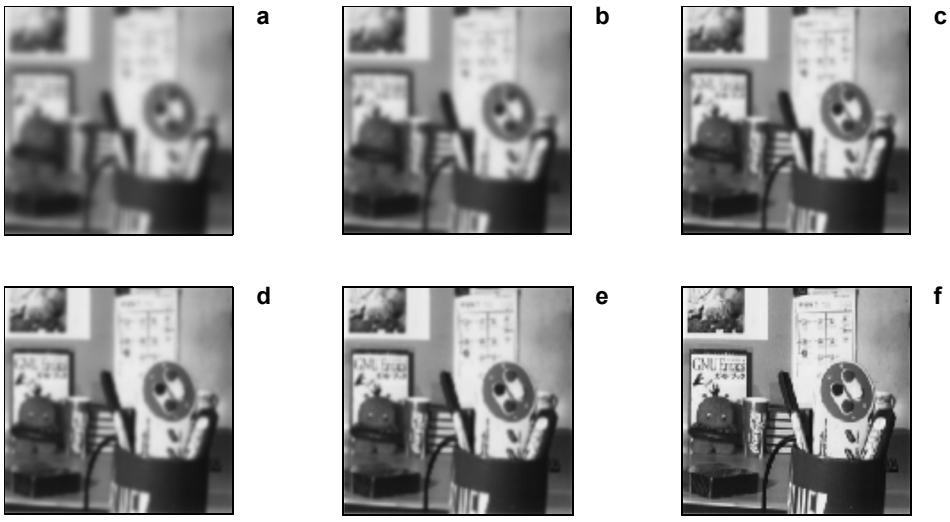

Fig. 2. Original and blurred versions of an image: radius = 2.0 (**a**), radius = 1.5 (**b**), radius = 1.0 (**c**), radius = 0.8 (**d**), radius = 0.5 (**e**), original (**f**).

T a b l e 1. Spatial frequency values for different blurred images in Fig. 2.

	Fig. 2**a**	Fig. 2**b**	Fig. 2**c**	Fig. 2**d**	Fig. 2**e**	Fig. 2**f**
SF	11.6565	14.5025	18.8483	21.5091	26.2995	46.8363

An image of size 128×128 is shown in Fig. 2**f**. Figures 2**a**–**e** show the upgrading of blurred versions of the image by decreasing the radius of Gaussian curvature (2.0, 1.5, 1.0, 0.8, 0.5, respectively). As can be seen from Tab. 1, when the image becomes clearer, the value of *SF* increases accordingly. Other experiments with image yield similar results. This suggests that spatial frequency can be used to evaluate the quality of chromosome, *i.e.*, fused image clarity.

4. Assessment measures

The performance measures used in this paper provide some quantitative comparison between different fusion schemes. The fusion approach may be objectively assessed with the use of suitable metrics.

4.1. Root mean square error

Our analytical performance studies were aimed to quantitatively assess image fusion performance in a straightforward manner. The root mean square error (RMSE), defined by the deviations between the reference image pixel value $R(i,j)$ and the fused image pixel value $F(i,j)$ (i,j denote pixel location), is computed as

$$\mathrm{RMSE} = \sqrt{\frac{\sum_{i=1}^{m}\sum_{j=1}^{n}\left[R(i,j)-F(i,j)\right]^2}{m\times n}} \tag{4}$$

where $m\times n$ is the input image size. If the value of 0 corresponds to the complete image reconstruction for block $m'\times n'$, it is a perfect image, which has been achieved through accurate reconstruction of multifocus to the reference image.

4.2. Entropy

Entropy is known to be a measure of the amount of uncertainty about the image. It is then given by

$$H = -\sum_{i=0}^{L-1} p_i \log_2 p_i \tag{5}$$

where L is the number of graylevels. Note that

$$p_i = \frac{\text{number of pixels } D_i \text{ of each graylevel } i}{\text{number of pixels } D \text{ in the image}}.$$

4.3. Mutual information

Mutual information is a measure that determines how much information is obtained from the fusion of input images. We use this measure as the fourth evaluation parameter to assess the performance of different image fusion algorithms;

$$MI(R, F) = \sum_{i_1=0}^{L-1} \sum_{i_2=0}^{L-1} p_{R,F}(i_1, i_2) \log_2 \frac{p_{R,F}(i_1, i_2)}{p_R(i_1) p_F(i_2)} \tag{6}$$

where $p_{R,F}$ indicates the normalized joint graylevel histogram of images R and F, p_R and p_F are the normalized marginal histograms of the two images. Here

$$p_{R,F}(i_1, i_2) = \frac{D(i_1, i_2)}{\sum_{i_1 i_2} D(i_1, i_2)}$$

where $D(i_1, i_2)$ is the number of pixel pairs at corresponding image graylevel (i_1, i_2), and $\sum_{i_1 i_2} D(i_1, i_2)$ is the total number of pixel pairs of the registered images. The normalized marginal histograms are counted like:

$$p_R(i_1) = \sum_{i_2} p_{R,F}(i_1, i_2), \quad p_F(i_2) = \sum_{i_1} p_{R,F}(i_1, i_2).$$

Notice that MI measures the reduction in uncertainty about the reference image due to the knowledge of the fused image, and so a larger MI is preferred. Another property of MI is just the following [20]

$$MI(A, A) = H(A). \tag{7}$$

This property allows ensuring a better decision of image reconstruction.

5. Example results of test images

Illustrative example is provided here under controlled conditions which allow meaningful performance comparisons of the various schemes.

In this example it is assumed that the images to be fused will come from a single sensor that produces fully registered images. In our study, we consider two blurring cases in more detail. In one case, the areas of two objects are not overlapped blurred, just like in Fig. 3. Figure 5 shows another case where areas of two objects are overlapped blurred.

In our experiments, we first apply our algorithm described in Sec. 3 to the images of Fig. 3**a** and **b**. In one image, the focus is on the forward. In the other image, the focus is on the backward. Experiment is performed on a 256-level image of size

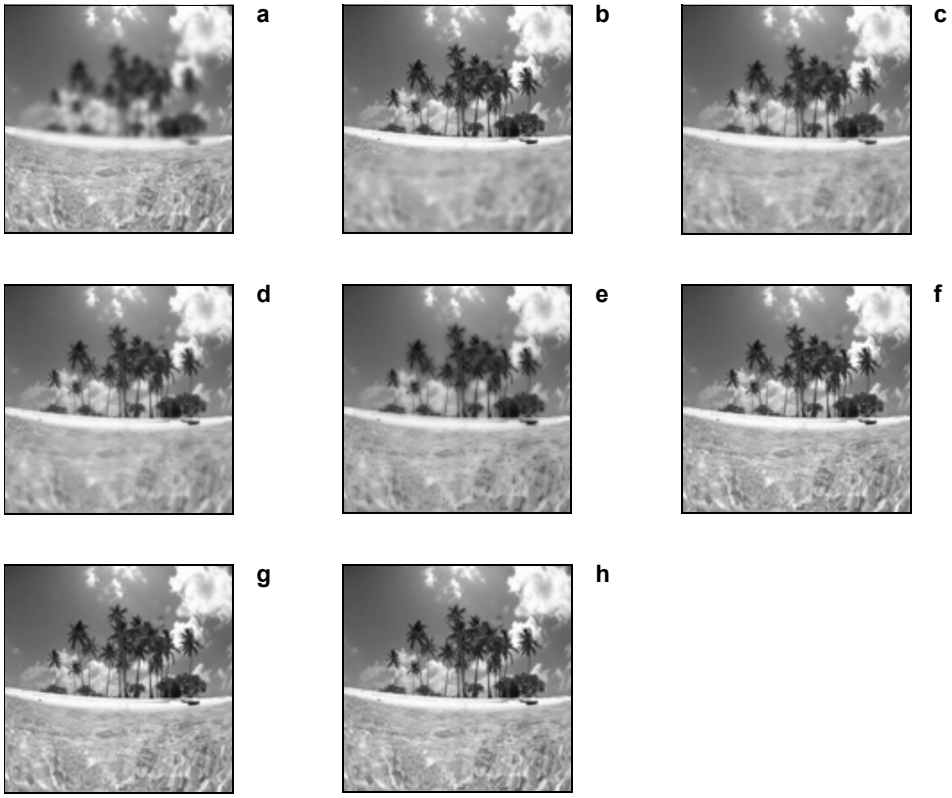

Fig. 3. Example of image fusion (without overlapped blurred regions). A pair of registered images with different focus points (**a**, **b**); the result of fusion obtained by weighted average (**c**); fused image obtained by the Laplacian pyramid (level = 3) (**d**); fused image obtained by RoLP pyramid (level = 3) (**e**); fused image obtained by DWT (db8, level = 3) (**f**); reference image (**g**); reconstructed output image obtained by GA algorithm (folding times 4 for 7×42 block) (**h**).

128×128 (Fig. 3**g**), with good-focus everywhere. This image is used as a benchmark with which the fusion algorithms are compared.

To verify the proposed optimized approach, five fusion algorithms are tested for objective performance evaluation applied to this pair of multifocus registered imagery (see Fig. 3). Figure 3**c** performs the simplest method–weighted average. In Fig. 3**d**, Laplacian algorithm is performed with appropriate weights assigned to this pair of inputs respectively. Figure 3**e** employs Toet algorithm with a maximum absolute contrast node selection technique. In Fig. 3**f**, the fusion rule is defined by calculating the wavelet transform modulus maxima using Daubechies 8 filter [21]. Figure 3**h** implements the new algorithm operation. The parameters of our genetic algorithm are: the reference population $N = 10$, the crossover ratio $P_c = 0.8$, the mutation ratio $P_m = 0.1$ and the folding times are 12.

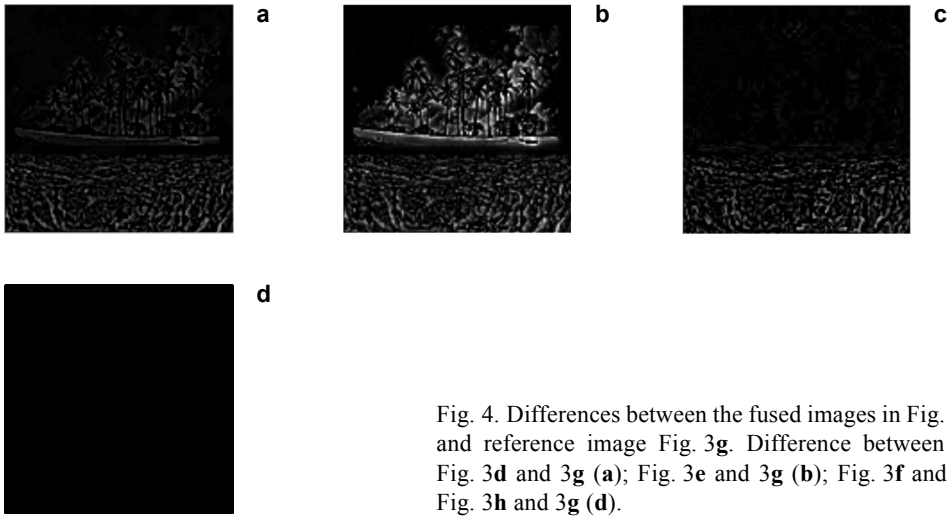

Fig. 4. Differences between the fused images in Fig. 3**d**–**f**, **h** and reference image Fig. 3**g**. Difference between image: Fig. 3**d** and 3**g** (**a**); Fig. 3**e** and 3**g** (**b**); Fig. 3**f** and 3**g** (**c**); Fig. 3**h** and 3**g** (**d**).

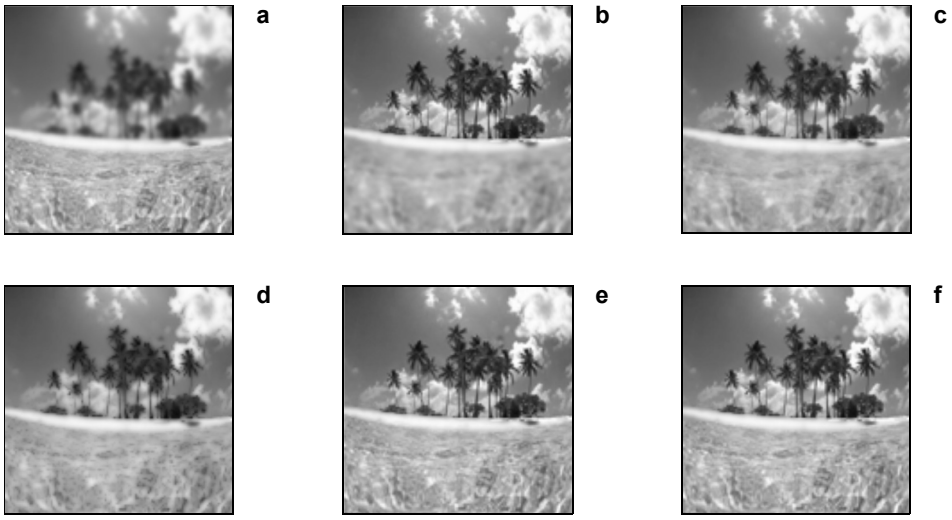

Fig. 5. Example of image fusion (with overlapped blurred regions). Images to be fused (**a**, **b**); fused image obtained by: the Laplacian pyramid (level = 3) (**c**); RoLP pyramid (level = 3) (**d**); DWT (db8, level = 3) (**e**); GA algorithm (folding times 6 for 76×52 block) (**f**).

Figure 5 shows the second case when the blurred regions are overlapped. A thorough comparison of the four approaches for multifocus image fusion is discussed in our research.

A clearer comparison can be made by examining the differences between the fused and reference image (Figs. 4 and 6). The difference is clearly visible. It can be seen

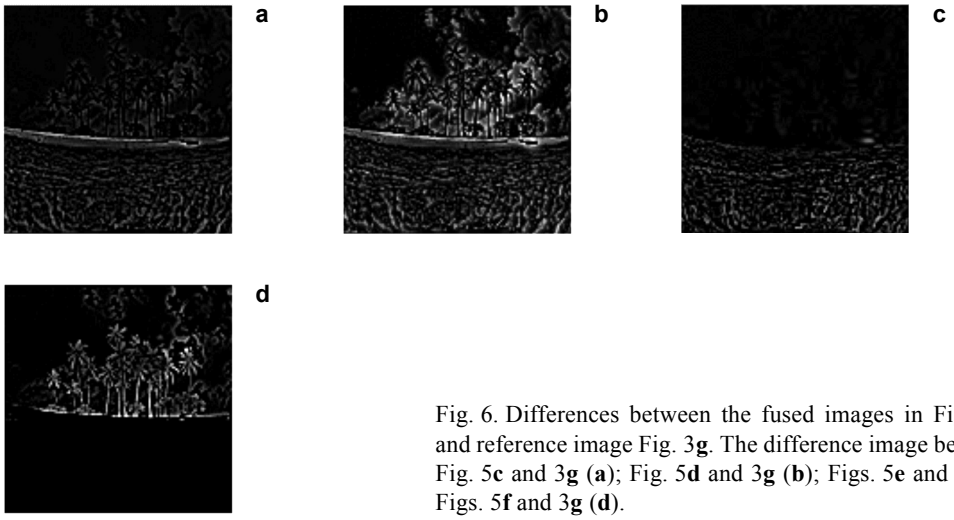

Fig. 6. Differences between the fused images in Fig. 5**c**–**f** and reference image Fig. 3**g**. The difference image between: Fig. 5**c** and 3**g** (**a**); Fig. 5**d** and 3**g** (**b**); Figs. 5**e** and 3**g** (**c**); Figs. 5**f** and 3**g** (**d**).

from Fig. 4**d** (completely dark) that unlike other fused images the reconstructed image produced by GA is optimal. It is a perfect restoration of the source images. It can also be seen from Fig. 6**d** that the fused image produced by GA is basically a combination of the well-focused parts in the source images.

At the same time, this illustrative example is provided here for some quantitative comparison of two cases in Tabs. 2 and 3. Very clearly, the results convincingly

T a b l e 2. Comparison of different schemes (no overlapped blurred objects).

	RMSE	*H*	*MI*
Average	6.1045	7.5031	4.1377
Laplacian	6.1094	7.5254	4.0564
RoLP	10.8447	7.5428	4.3430
Wavelet	1.5911	7.5976	5.2720
GA	0	7.6002	7.6002

T a b l e 3. Comparison of different schemes (overlapped blurred objects).

	RMSE	*H*	*MI*
Laplacian	6.9293	7.5246	3.9200
RoLP	10.5560	7.5358	4.3818
Wavelet	3.8021	7.5991	5.1072
GA	3.7453	7.6013	7.3244

demonstrate that Fig. 3**h** (from GA method) is the reconstructed image, more clear than other figures, which entropy equals mutual information, and RMSE equals 0. Figure 3**h** can be considered as the perfect fusion result. Many of those multiresolution methods have approximately 2% to 3% reconstruction error. The proposed approach, which has effectively achieved zero reconstruction error in the first case, is used in this article. This GA method directly produces the desired image of the source images. From this genetic search, using objective evaluation measures makes the computer choose the best fused image automatically. It is found that the genetic scheme achieves the best result when compared with other methods.

In the second case, Fig. 5**f** is the most clear fused image achieved by GA method, whose entropy and mutual information are relatively improved, and RMSE is relatively reduced. By means of *MI*, features of visual information from input images and new fused images can be measured.

Overall the presented approach explicitly shows better fusion performance, both esthetically and numerically. Note that the level of agreement between subjective and objective results is particularly high. Moreover, in contrast to previous methods, the technique presented here is, in principle, parameter free. The effectiveness of our method can be seen from this.

Better fusion results, both visually and quantitatively based on the performance measure, have been achieved by using the GA algorithm.

In addition to the above image, we have performed more image experiments and have obtained the reconstructed or optimized fusion results.

6. Digital camera multifocus image application

In most previous studies, the images to be fused are assumed to be registered. The sensors used for image fusion need to be accurately coaligned, so that their images will be in spatial registration. In our research, we take the assumption that we have the source images. Given an input image and a reference image, an error image that is uncorrelated with the reference image can be computed.

Another case, *i.e.*, multifocus digital camera images, is an important issue that should be studied. The reference image, *i.e.*, the ideal fusion result, however, is not available, so only a subjective visual comparison is intended here. Because these images have not the reference image, so no ideal fusion result is known. The real camera used for the acquisition of two images has a single trace in a 2-D plane defined by the degree of blurring of the foreground and background objects. For example, when the foreground is in focus, the background is blurred to some extent, and *vice versa*.

Take the "Disk" images as an example. Figure 7 shows a pair of digital camera images. Recall that the focus in Fig. 7**a** is on the clock while that in Fig. 7**b** is on the shelf. Figure 7**c** is the image obtained using the auto-focus function of the camera. Fusion results obtained using DWT and GA are shown in Figs. 7**d**–**f**. Obviously, image fusion algorithms perform better than the camera's auto-focus function. It can be seen

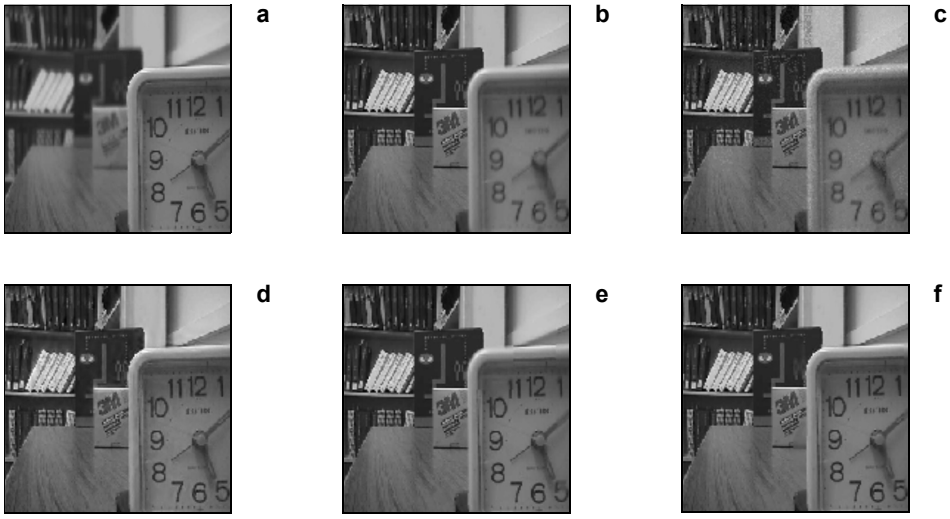

Fig. 7. Example of digital camera image fusion. A pair of digital camera images with different focus points (**a**, **b**); auto-focus image (**c**); fused image obtained by DWT (db8, level = 3) (**d**); fused image obtained by GA algorithm (folding times 1, for 117×48 block) (**e**), fused image obtained by GA algorithm (folding times 1, for 34×25 block) (**f**).

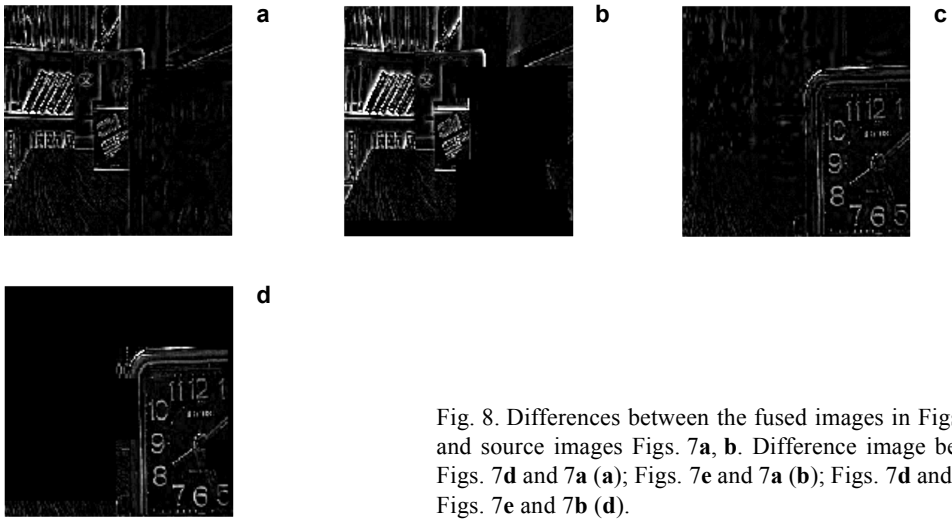

Fig. 8. Differences between the fused images in Figs. 7**d**, **e** and source images Figs. 7**a**, **b**. Difference image between: Figs. 7**d** and 7**a** (**a**); Figs. 7**e** and 7**a** (**b**); Figs. 7**d** and 7**b** (**c**); Figs. 7**e** and 7**b** (**d**).

from Figs. 7**e** and **f** that the fused image produced by GA is basically a combination of the good-focus clock and the good-focus shelf. In particular, notice that there is a slight movement of the books on the shelf and the pointers of the clock in Fig. 7**d**, and this affects the clarity. Because wavelet transform has not the characteristic of shift, that is the shift of signal brings about greater influence of the decomposition

coefficient. The use of GA solves the problem and we get legible fused images, so the result obtained by DWT appears to be worse. The GA produces very similar results in Figs. 7**e** and **f**, so will not be reported here.

Again, a clearer comparison of their performance can be made by examining the differences between the fused images and each source image (Fig. 8). Notice that it is completely dark in the left part in Fig. 8**d**. Anyhow the GA method has produced a better fusion result than DWT method.

Experimental results show that this method outperforms the DWT-based approach, particularly when there are either object movement or registration problems in the source images.

Therefore, genetic search can pick excellence and discard low quality through blocks increasing or decreasing process, and look for the best matching value and perform high quality answer.

7. Disscusion

Compared to the previous work, our method was being enhanced as the research progressed and has the following features:

1. While the previous works mainly deal with image fusion, we now pay more attention to the optimization procedure for the fused image. Their good performance appears to be due to two facts. One is that the human visual system is especially sensitive to local contrast changes. It can determine the definition of image object very well. The other is that multifocus image fusion may be viewed as an evolutionary process from one reference shape (raw image) to another shape (fused or reconstructed image). The GA algorithm is adaptive. Still, this is a robust and reliable image fusion technique with high speed.

2. Here, a comparative analysis of two cases of test images is provided. When the focus objects are not overlapped blurred, using this method one can achieve accurate reconstruction or optimized results of multifocus images compared to reference ones. This method may provide zero error as long as perfect registration in the multifocus images is concerned. When the focus objects are overlapped blurred, this method offers good performance outperforming conventional multiresolution Laplacian and wavelet transform algorithms.

3. From the first case it can also be expanded that the accurate reconstructed image could be achieved with different blurring radius or blurring kernel (such as Gaussian blurring or motion blurring, etc.) in the same multifocus image.

4. This method is easily to be extended to real camera images of multifocus. This is of practical significance. It can fuse the clear part into one image without alerting the characteristic of input images. It is independent of large variations in the global graylevel characteristics of the individual input images. Moreover, the technique may be readily applied to digital camera images of different focus as well as different size. It is shown that the method works well for both synthesized and real images.

5. Here, we consider the processing of just two source images; in fact the algorithm can be extended straightforwardly to handle more than two of them.

8. Conclusions

In this paper, we combine the idea of image blocks and genetic search strategies for pixel level multifocus image fusion. In this method, the size of image block was defined as chromosome. After crossover and mutation, the global optimal solution would be got. Whether the multifocus images are manually produced, or camera produced, experiments based on subjective and objective evaluation measures provide a marked improvement in the fused results compared with other multiresolution methods we considered. Therefore this method provides satisfactory results as far as fusion is concerned.

In conclusion, the GA method, relying on some genetic search factors, is a novel attempt to apply concepts coming from genetics to image processing, specifically multifocus images. We believe that further research on this topic is worthwhile and promising.

References

[1] VARSHNEY P.K., *Multisensor data fusion*, Electronics and Communication Engineering Journal **9**(6), 1997, pp. 245–53.

[2] BURT P.J., ANDELSON E.H., *The Laplacian pyramid as a compact image code*, IEEE Transactions on Communication **COM-31**(4), 1983, pp. 532–40.

[3] BURT P.J., ADELSON E.H., *Merging images through pattern decomposition*, Proceedings of the SPIE **575**, 1985, pp. 173–81.

[4] TOET A., VAN RUYVEN L.J., VALETON J.M., *Merging thermal and visual images by a contrast pyramid*, Optical Engineering **28**(7), 1989, pp. 789–92.

[5] TOET A., *Multiscale contrast enhancement with applications to image fusion*, Optical Engineering **31**(5), 1992, pp. 1026–31.

[6] BURT P.J., KOLCZYNSKI R.J., *Enhanced image capture through fusion*, [In] Proceedings of the 4th International Conference on Computer Vision 4, Berlin, Germany 1993, pp. 173–82.

[7] LIU Z., TSUKADA K., HANASAKI K., HO Y.K., DAI Y.P., *Image fusion by using steerable pyramid*, Pattern Recognition Letters **22**(9), 2001, pp. 929–39.

[8] DAUBECHIES I., *Ten Lectures on Wavelets*, Society for Industrial and Applied Mathematics/ CBMS-NSF regional conference series in applied mathematics 61, Philadelphia 1992.

[9] HUNTSBERGER T., JAWERTH B., *Wavelet based sensor fusion*, Proceedings of the SPIE **2059**, 1993, pp. 488–98.

[10] MALLAT S.G., *A theory for multiresolution signal decomposition: the wavelet representation*, IEEE Transactions on Pattern Analysis and Machine Intelligence **11**(7), 1989, pp. 674–93.

[11] MALLAT S.G., *Wavelets for a vision*, Proceedings of the IEEE **84**(4), 1996, pp. 604–14.

[12] ZHANG Z., BLUM R.S., *A categorization of multiscale-decomposition-based image fusion schemes with a performance study for a digital camera application*, Proceedings of the IEEE **87**(8), 1999, pp. 1315–26.

[13] CHIBANI Y., HOUACINE A., *On the use of redundant wavelet transform for multisensor image fusion*, [In] Proceedings of the 7th IEEE International Conference on Electronics, Circuits and Systems, Jounieh, Lebanon 2000, pp. 442–5.

[14] LI S.T., WANG Y.N., ZHANG C.F., *Feature of human vision system based multi-focus image fusion*, Acta Electronica Sinica **29**(12), 2001, pp. 1699–701.
[15] LI S.T., KWOK J.T., WANG Y.N., *Multifocus image fusion using artificial neural networks*, Pattern Recognition Letters **23**(8), 2002, pp. 985–97.
[16] HUANG J.W., SHI Y.Q., DAI X.H., *A segmentation-based image coding algorithm using the features of human vision system*, Journal of Image and Graphics **4**(5), 1999, pp. 400–4.
[17] GOLDBERG D.E., *Genetic Algorithms in Search, Optimization and Machine Learning*, Addison -Wesley Publishing Company, Redwood City, CA 1989.
[18] de PEUFEILHOUX R., *Genetic fusion of registered images*, Proceedings of the SPIE **1607**, 1991, pp. 380–4.
[19] XU Y.L., BI D.Y., MAO B.X., MA L.H., *A genetic search algorithm for motion estimation*, Journal of Image and Graphics **6**(2), 2001, pp. 164–7.
[20] MAES F., COLLIGNON A., VANDERMEULEN D., MARCHAL G., SUETENS P., *Multimodality image registration by maximization of mutual information*, IEEE Transactions on Medical Imaging **16**(2), 1997, pp. 187–98.
[21] LI H., MANJUNATH B.S., MITRA S.K., *Multisensor image fusion using the wavelet transform*, Graphical Models and Image Processing **57**(3), 1995, pp. 235–45.

Received June 1, 2005